Transport phenomena in alkaline direct ethanol fuel cells for sustainable energy production

L. An[a]* and T.S. Zhao[b]*

[a]Department of Mechanical Engineering, The Hong Kong Polytechnic University, Hung Hom, Kowloon, Hong Kong SAR, China

[b]Department of Mechanical & Aerospace Engineering, The Hong Kong University of Science and Technology, Clear Water Bay, Kowloon, Hong Kong SAR, China

*Corresponding authors.

[a]Email: liang.an@polyu.edu.hk (L. An)

[b]Email: metzhao@ust.hk (T.S. Zhao)

Abstract

Alkaline direct ethanol fuel cells (DEFC), which convert the chemical energy stored in ethanol directly into electricity, are one of the most promising energy-conversion devices for portable, mobile and stationary power applications, primarily because this type of fuel cell runs on a carbon-neutral, sustainable fuel and the electrocatalytic and membrane materials that constitute the cell are relatively inexpensive. As a result, the alkaline DEFC technology has undergone a rapid progress over the last decade. This article provides a comprehensive review of transport phenomena of various species in

this fuel cell system. The past investigations into how the design and structural parameters of membrane electrode assemblies and the operating parameters affect the fuel cell performance are discussed. In addition, future perspectives and challenges with regard to transport phenomena in this fuel cell system are also highlighted.

1. Introduction

Direct ethanol fuel cells (DEFC), which promise to be a clean and efficient energy production technology, have recently attracted worldwide attention, primarily because ethanol is a carbon-neutral, sustainable fuel and possesses many unique physicochemical properties including high energy density and ease of transportation, storage as well as handling [1-6]. However, conventional DEFCs that use acid proton exchange membranes (PEM) and precious metal catalysts result in rather low performance [7], primarily because it is difficult to oxidize ethanol in acid media. It has been recently demonstrated that when the acid electrolyte was changed to alkaline one, i.e.: hydroxide exchange membrane (HEM) and hydroxide exchange ionomer (HEI), the cell performance could be substantially improved mainly due to the faster kinetics of both the ethanol oxidation reaction (EOR) and oxygen reduction reaction (ORR) in alkaline media, even with cheaper materials including alkaline membranes and non-precious-metal electrocatalysts [8]. Therefore, alkaline DEFCs have attracted ever-increasing attention in recent years [9-16].

The conventional architecture design of alkaline DEFCs that purely relies on an HEM and HEIs to conduct ions exhibited extremely low performance [17], which is primarily attributed to the low conductivity of state-of-the-art HEMs and corresponding HEIs. As such, the past efforts with regard to the research and

3

development of alkaline DEFCs are mainly made to developing high-conductivity

HEMs and HEIs, as well as highly electrocatalytic materials for both the EOR and

ORR [18, 19]. However, it has been demonstrated that, even using existing HEM and

HEI, as well as electrocatalysts (for EOR and ORR), an introduction of an alkali

(NaOH/KOH) to fuel solution enables alkaline DEFCs to yield extremely high

performance [20, 21]. Such an improvement in the cell performance is basically

attributed to the added alkali, which not only allows a drastic increase in the ionic

transport rate through the membrane electrode assembly (MEA) [22, 23], but also

further enables the kinetics of the electrochemical reactions to be speeded up [24].

The absence of alkali in the fuel solution has demonstrated extremely low

performance [19]. Past review articles regarding alkaline DEFCs are mainly focused

on the development of electrocatalysts and electrocatalytic mechanisms [25-31],

HEMs and HEIs [27, 30, 32, 33], as well as single cell design and performance

comparison [21, 27, 28, 30, 31]. This article provides a comprehensive review of the

past research on transport phenomena of various species through the MEA in this fuel

cell system. The remaining parts of this review are organized as follows: Section 2

presents a general description of transport processes; Sections 3 - 5 review the

transport of various species through the MEA; and Section 6 gives a summary and

perspective.
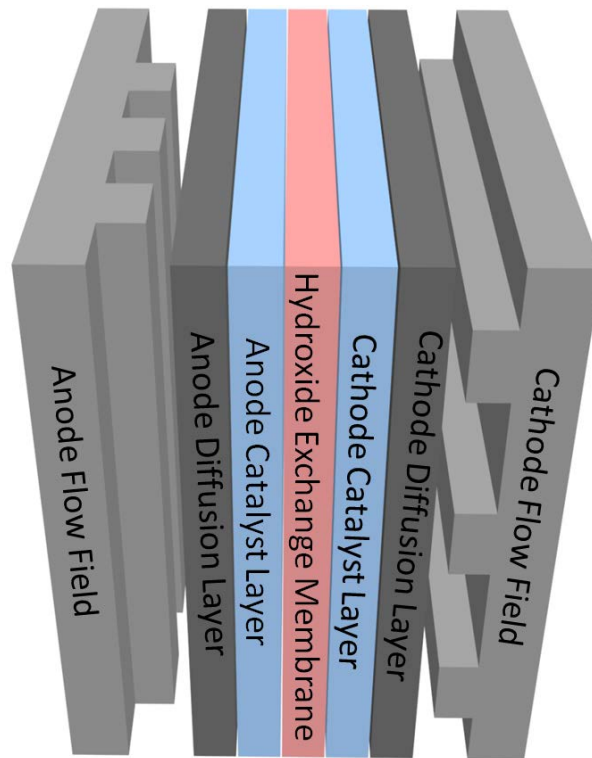
Fig. 1 A typical alkaline direct ethanol fuel cell (DEFC).

2. General description

Fig. 1 shows a typical alkaline DEFC structure, in which the MEA consists of an anode and a cathode separated by an HEM. On the anode, the fuel solution containing ethanol and alkali flows into the anode flow channel and transports through the anode diffusion layer (DL) to the anode catalyst layer (CL), where theoretically ethanol will be oxidized to produce electrons, water, and carbon dioxide according to [21]:

$$CH_3CH_2OH + 12OH^- \rightarrow 2CO_2 + 9H_2O + 12e^- \qquad E_a^o = -0.74V \quad (1)$$

Although ethanol can be completely oxidized into carbon dioxide on some electrocatalysts in alkaline media [19], the main product of the EOR on Pd-based electrocatalysts is acetate and thus the anodic reaction becomes [2]

$$CH_3CH_2OH + 5OH^- \rightarrow CH_3COO^- + 4e^- + 4H_2O \qquad E_a^o = -0.74V \quad (2)$$
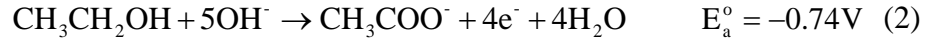
The water in the anode will transport through the membrane and arrive the cathode, while the produced electrons transport through the external circuit to the cathode.

On the cathode, the oxygen transports through the cathode DL to the cathode CL, where oxygen will react with electrons and water to produce hydroxide ions:

$$O_2 + 2H_2O + 4e^- \rightarrow 4OH^- \qquad E_c^o = 0.40V \quad (3)$$

The hydroxide ions in the cathode migrate through the HEM to the anode for the EOR. The combination of the EOR given by Eq. (2) and the ORR given by Eq. (3) results in an overall reaction:

$$CH_3CH_2OH + O_2 + OH^- \rightarrow CH_3COO^- + 2H_2O \qquad E^o = 1.14V \quad (4)$$

It should be noted that although the overall reaction of the present alkaline DEFC (with an added alkali) is the same with that of the conventional one (alkali-free), the presence of both M^+ ions and OH^- ions due to the introduction of the alkali (MOH) in the fuel solution creates an anion-cation co-existing system, thereby showing more complicated transport phenomena [34]. In the following sections, we discuss the transport characteristics of various species and review the past investigations on the transport phenomena in alkaline DEFCs.

3. Transport phenomena in the anode

As mentioned earlier, ethanol in the fuel solution flows into the anode flow channel

6

and transports through the anode DL to the anode CL. Hence, the operating parameters and anode structural design parameters will affect the transport process of ethanol in the cathode. A low ethanol concentration will cause the transport loss of ethanol and thus lower the anode performance. A high ethanol concentration will cause two issues: 1) the majority of the reaction sites will be occupied by ethanol, which leads to a decrease in the reaction sites occupied by hydroxide ions and thus increases the anode activation loss [19]; and 2) an increase in the ethanol crossover rate still reduces the fuel utilization efficiency, although there would be no mixed-potential problem if the ethanol-tolerant electrocatalysts will be employed at the cathode. Therefore, it is critically important to achieve an appropriate ethanol concentration in the anode CL.
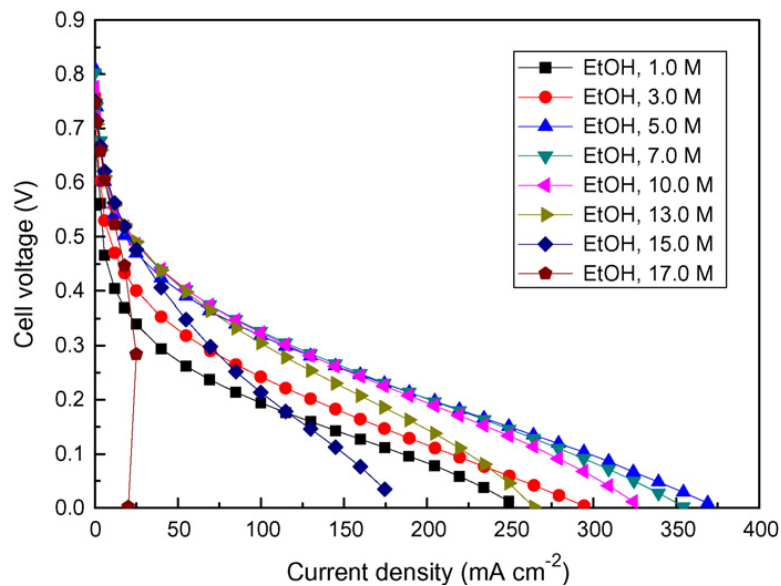
(a)
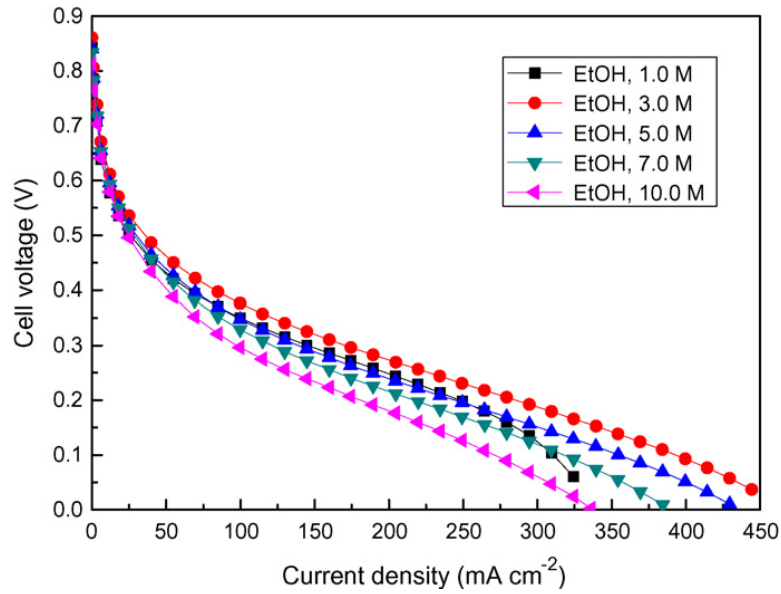
(b)
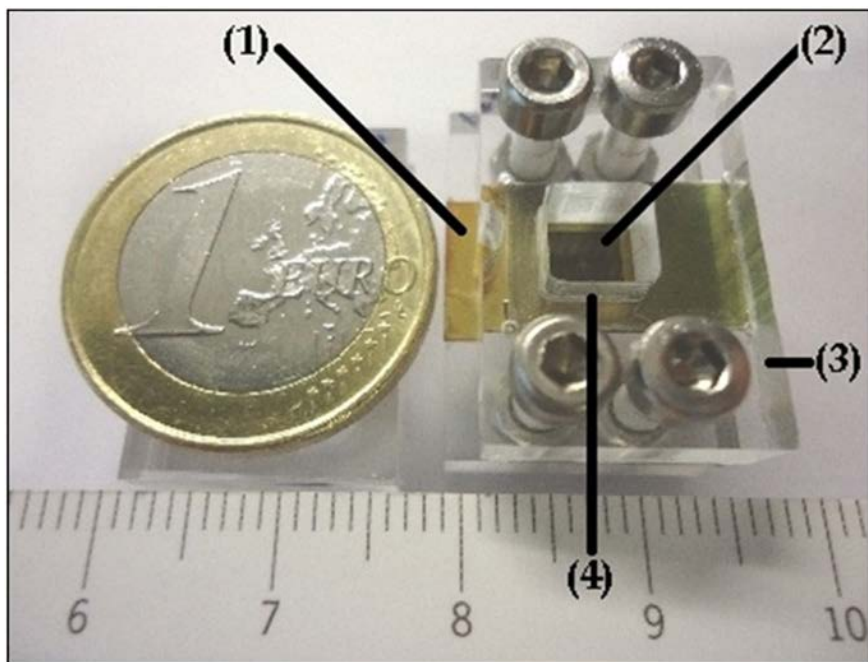
(c)

Fig. 2 Effect of the ethanol concentration on the cell performance: (a) 1.0 M KOH; (b)

5.0 M KOH [24]. (c) The fabricated micro-DEFC via using micro-technologies: (1)

Si-based current collector; (2) micro-fabricated channels; (3) methacrylate case holder;

and (4) MEA [37] (Reproduced with permission from IOP Publishing).

3.1. Effect of the ethanol concentration

The ethanol concentration in the fuel solution is an important parameter that can be varied to maintain an appropriate ethanol concentration in the anode CL. Hence, the effect of the ethanol concentration on the cell performance has been extensively studied [24, 35, 36, 37, 38]. Li et al. [24] investigated the effect of the ethanol concentration on the cell performance, as shown in Figs. 2a and 2b. It was found that the cell resulted in the highest performance with an ethanol concentration of 5.0 M (in 1.0 M KOH). It was also found that the high-concentration ethanol created a barrier for the transfer of hydroxide ions, increasing the internal resistance and thus lowering the performance. The similar phenomenon was also found when experiments were performed with a KOH concentration of 5.0 M. Verjulio et al. [37] developed a micro-DEFC via using micro-technologies to fabricate the current collectors, as shown in Fig. 2c. The fuel cell was operated by using ethanol and KOH mixed solution as fuel and the ambient air as oxidant. They tested the fuel cell with various ethanol concentrations ranging from 1.0 M to 4.0 M (containing 4.0 M KOH in the fuel solution) at room temperature and found that the highest power density (100 μW cm^{-2} at 0.47 V) was obtained when operated with an ethanol concentration of 4.0 M.

In summary, increasing the ethanol concentration leads to an increase in the transport rate of ethanol in the anode, thereby improving the cell performance.

However, when the ethanol concentration is too high, the majority of reaction sites are occupied by ethanol, blocking the adsorption of hydroxides ions on the reaction sites and thus lowering the EOR kinetics and, in turn, decreasing the cell performance. For a given fuel cell design, therefore, there exists an optimal ethanol concentration, at which the cell yields the highest power density.

3.2. Effect of the anolyte flow rate

The flow rate of the anolyte can also influence the transfer of ethanol in the anode. Increasing the anolyte flow rate can enhance the transport of ethanol, as a result of the fact that a decrease in the difference of the ethanol concentration between the inlet and the outlet results in a more uniform distribution of ethanol over the electrode [86]. Hence, the effect of the anolyte flow rate has been studied [2, 24]. For example, Li et al. [24] investigated the effect of the anolyte flow rate ranging from 0.3 mL min^{-1} to 3.0 mL min^{-1} at a fixed operating temperature of 40°C. It was found that the cell performance was improved with increasing anolyte flow rate due to the enhanced transport of ethanol. They also suggested that the effect became insignificant when the ethanol concentration was higher than 1.0 M.

3.3. Effect of the anode diffusion layer

In addition, the transport process of ethanol is also affected by the anode structural design parameters. It should be mentioned that the DL is not only to facilitate the

transport from the flow channel to the CL (in the through-plane direction), but also to enhance the transport in the in-plane direction to make the reactants more uniformly distribute over the electrode [86]. An et al. [38] studied the effect of the structural design parameters, including the thickness and porosity of the anode DL, on the cell performance, as shown in Figs. 3a and 3b. It was found that with increasing the anode DL thickness, the cell performance was gradually decreased. From the transport point of view, therefore, the thinner anode DL is preferred due to the higher reactant delivery rate and product removal rate. It was also found that with increasing the DL porosity from 73% to 98%, the transport of ethanol was gradually enhanced. As such, the nickel foam with a porosity of 95% is generally employed in this fuel cell system. It should be noted that the DL functions as not only a reactant distributor, but also an electron collector and a CL supporter. A higher porosity means a larger electron transport resistance and a worse mechanical property. Therefore, there exists an optimal porosity.
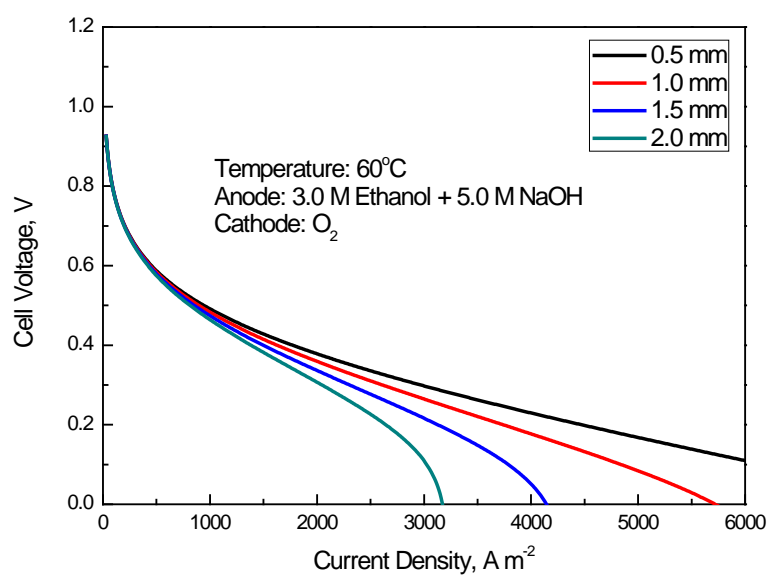
(a)
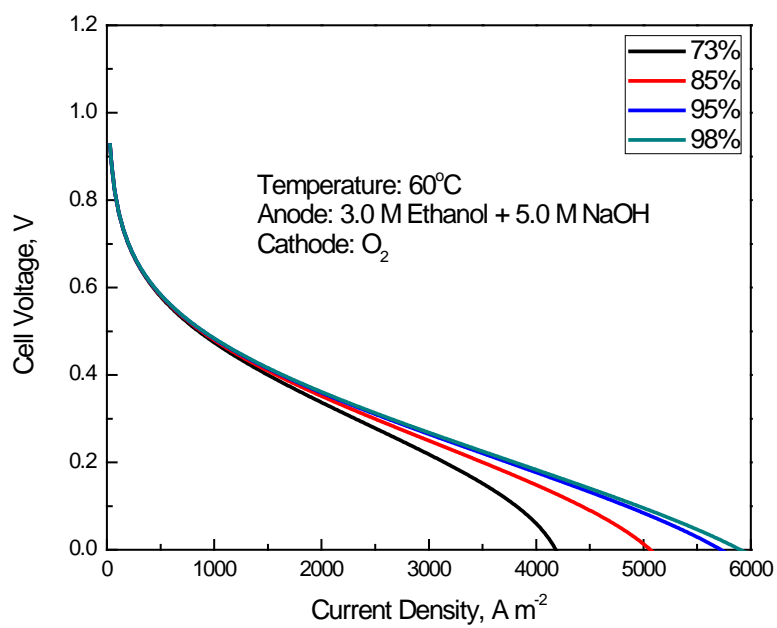
(b)
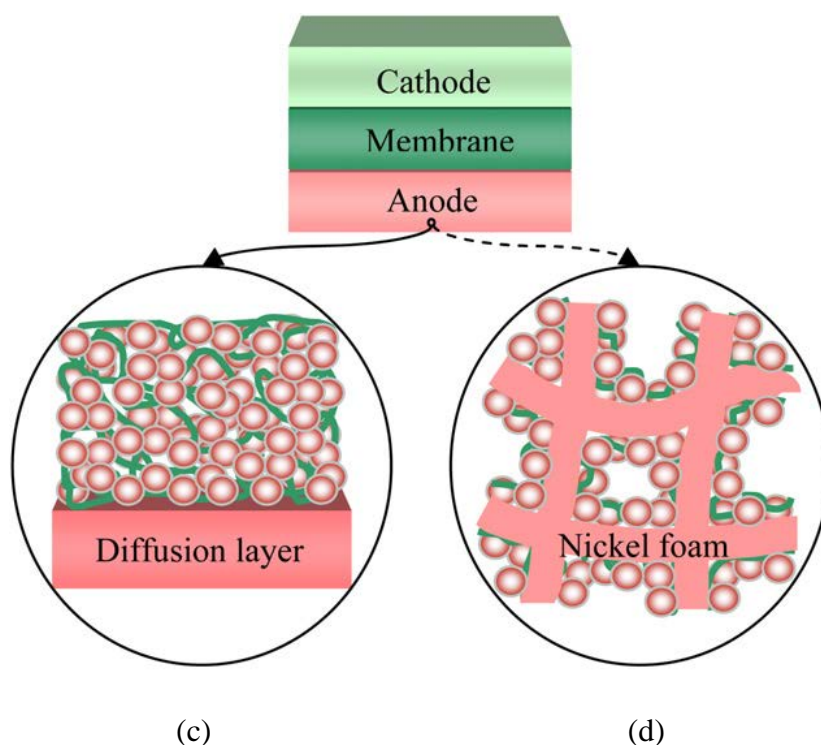
Fig. 3 Effect of structural parameters on the performance: (a) thickness; (b) porosity [38]. Anode structures: (c) the conventional one; and (d) the integrated one [36].

3.4. Effect of the anode catalyst layer

The transport of ethanol in the anode is also affected by the ionomer/binder [2, 17]. Li et al. [17] compared a hydroxide-conducting ionomer (A3) and a neutral polymer binder, polytetrafluoroethylene (PTFE), and demonstrated that the use of the PTFE in preparing the anode CL yielded better performance than the A3 ionomer. It was found that the use of the A3 ionomer resulted in a film-like CL; while the use of the PTFE binder formed a porous CL. The porous microstructure formed by using PTFE binder enables reaction sites more accessible to the reactants, thereby upgrading the cell performance. Due to the unique microstructure and good durability, the PTFE binder

is widely used in preparing the CLs in this fuel cell system.

3.5. Effect of the anode structure design

Li et al. [36] proposed an anode structure consisting of a nickel foam layer (functioning as DL) with thin catalyst films (functioning as CL) deposited onto the skeleton of the nickel foam, as shown in Figs. 3c and 3d. It was found that compared to the conventional electrode (that has separated CL and DL), the use of the integrated one significantly improved the cell performance, exhibiting a peak power density of 130 mW cm^{-2}. Chetty et al. [39] prepared an integrated electrode via the thermal decomposition of platinum-based binary and ternary catalysts on titanium mesh. The performance test showed that the use of the mesh-based electrode as the anode of alkaline DEFCs resulted in a comparable performance with the conventional one. Wang et al. [40] fabricated a three-dimensional Pd electrode via electrodepositing Pd nanoparticles on the nickel foam, as shown in Fig. 4. The electrochemical properties toward the EOR of the as-prepared electrode were studied by cyclic voltammetry (CV). It was showed that the peak current density of the Pd/nickel foam electrode was 107.7 mA cm$^{-2,}$ which was about 8 times higher than that of Pd-film electrode. The improved activity and stability of the Pd/nickel foam electrode makes it a suitable electrode for the anode of alkaline DEFCs. In summary, it is suggested that the anode structure that integrates a DL and a CL is more suitable for this fuel cell system.
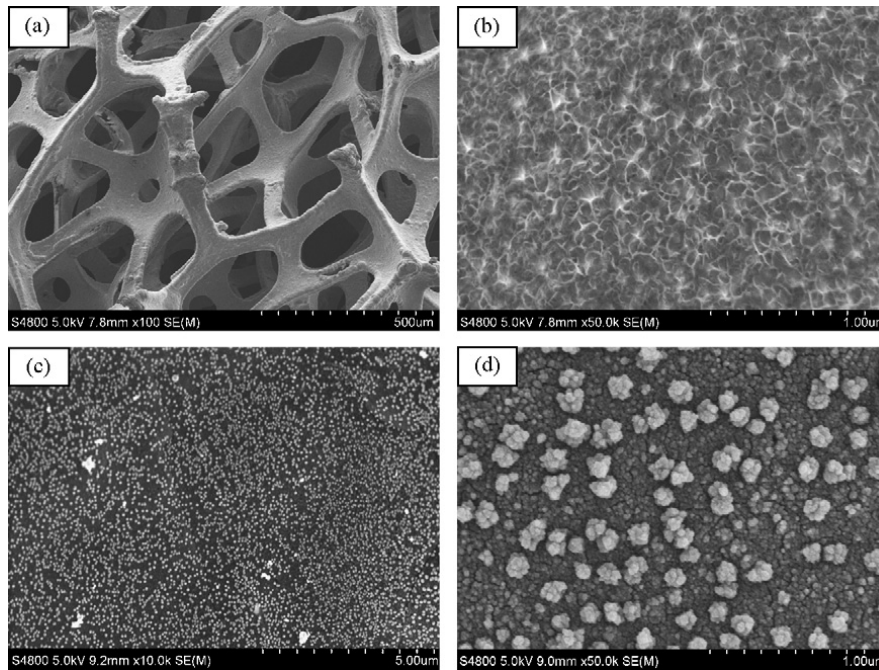
Fig. 4 A three-dimensional Pd electrode [40].

4. Transport phenomena through the membrane

In fuel cells, a membrane has to be used to separate the anode and the cathode, physically preventing the short circuit, and to conduct ions functionally forming ionic current. In addition, the membranes are also permeable to the species in the anolyte, including ethanol, alkali and water, so that they can transport through the membrane to the cathode. It should be noted that in principle, the ionic current in alkaline fuel cells is created by conducting hydroxide ions from the cathode to the anode, which is opposite to that (protons) in acid fuel cells. Hence, the direction of the electro osmotic drag (EOD) in this fuel cell system is from the cathode to the anode, thereby reducing the permeation rate of species to the cathode. It indicates that the species crossover in alkaline fuel cells is not serious as that in acid fuel cells. The following subsections

15

will discuss the transport mechanisms of various species through the membrane.

4.1. Ethanol transport through the membrane (ethanol crossover)

As mentioned earlier, ethanol transporting through the membrane (ethanol crossover) may cause two technical problems. First, ethanol may be oxidized to form the parasitic current, leading to a mixed potential on the cathode, although the electrocatalysts on the cathode are almost inactive to ethanol so that the mixed-potential problem is insignificant in this fuel cell system. Second, the ethanol crossover definitely results in a waste of fuel, decreasing the utilization efficiency. Therefore, the rate of ethanol crossover should be reduced to increase the fuel utilization efficiency. Generally, there are three mechanisms for ethanol transport through the membrane.

(i) Diffusion by the ethanol concentration gradient:

$$J_{\mathrm{D}} = D_{\mathrm{e, m}} \frac{(C_{\mathrm{acl/m}} - C_{\mathrm{ccl/m}})}{\delta_{\mathrm{m}}} \tag{5}$$

where $D_{\mathrm{e, m}}$ represents the effective diffusivity of ethanol; δ_{m} is the membrane thickness; $C_{\mathrm{acl/m}}$ and $C_{\mathrm{ccl/m}}$ stand for ethanol concentrations at two interfaces.

(ii) Electro-osmotic drag (EOD) by the hydroxide-ion migration:

$$J_{\mathrm{EOD}} = X_{\mathrm{ccl/m}} n_{\mathrm{d}} \frac{i}{F} \tag{6}$$

where n_{d} represents the EOD coefficient of water; and $X_{\mathrm{ccl/m}}$ is the ethanol molar fraction at the interface.

(iii) Convection by the liquid pressure gradient:

$$J_{\mathrm{C}} = \frac{C_{\mathrm{acl/m}} K_{\mathrm{m}} \Delta p}{\delta_{\mathrm{m}} \mu} \tag{7}$$

Therefore, the total flux of ethanol through the membrane can be expressed as:

$$J_{\mathrm{ec}} = J_{\mathrm{D}} + J_{\mathrm{C}} - J_{\mathrm{EOD}} = D_{\mathrm{e,m}} \frac{(C_{\mathrm{acl/m}} - C_{\mathrm{ccl/m}})}{\delta_{\mathrm{m}}} + \frac{C_{\mathrm{acl/m}} K_{\mathrm{m}} \Delta p}{\delta_{\mathrm{m}} \mu} - X_{\mathrm{ccl/m}} n_{\mathrm{d}} \frac{i}{F} \tag{8}$$

Based on Eq. (8), it can be seen that ethanol crossover is strongly dependent of diffusion across the membrane. First, the ethanol crossover rate could be decreased by reducing the ethanol permeability of the membrane. For this reason, the ethanol permeabilities of various alkaline membranes have been extensively measured [41-45]. Varcoe et al. [41] investigated the ex-situ ethanol permeabilities of two alkaline membranes and found that the ethanol permeabilites were lower than the methanol permeabilities. Hou et al. [42] prepared an HEM for alkaline DEFCs via doping KOH in polybenzimidazole (PBI) membrane, i.e.: alkali-doped PBI membrane (APM). The ethanol permeability through this membrane was 6.5×10^{-7} cm^2 s^{-1}, which was smaller than the Nafion membrane. They explained that there were hydrophilic groups (–SO$_3$H) in the Nafion membrane so that the membrane was swollen more significantly than the present membrane when immersed in the ethanol solution. As such, the less expanded space among PBI backbones probably resulted in a lower value in the ethanol permeability. Leykin et al. [43] proposed a method to measure the ethanol permeability of polymeric membranes in alkaline media. The rate

of the ethanol crossover through KOH-doped poly[2,2-(4,4-diphenylether)-5,5-bibenzimidazole] was investigated at various alkali concentrations. It was shown that the ethanol permeability was 8.6×10^{-8} cm^2 s^{-1} in 3.0 M KOH, which would be further decreased with the alkali concentration. Also, they claimed that the proposed method could be expanded to measuring the alcohol permeabilities of the polymeric membrane in various aqueous solutions under the acid condition. Jung et al. [44] developed an anion exchange pore-filling membrane that offered low liquid fuel permeation rate while maintaining hydroxide-ion conduction rate. The striking feature of this membrane was that the exterior porous substrate suppressed swelling of the interior polyelectrolyte and controlled the inner water to be wholly bound water, even under fully humidified condition. It was proved that hydroxide ions could be conducted through bound water. They also clarified that this bound water effectively reduced permeation rate of liquid fuels. Recently, An et al. [45] investigated the ethanol permeabilities for three types of commercial membrane, i.e.: HEM (Tokuyama A201), APM (PBI membrane provided by Yick-Vic) and cation exchange membrane: CEM (Nafion 211), all of which were generally used in alkaline DEFCs. It was found that the ethanol permeabilities of the three membranes were in the similar range (1×10^{-7} cm^2 s^{-1}) at room temperature. It should be pointed out that the permeability measurement conducted in alkaline aqueous solution will provide

more reliable data than those done in pure water, because the alkali doping process is encountered when immersed in alkaline solution, which definitely affects alcohol permeability [43]. Second, the ethanol crossover rate can also be reduced by increasing the membrane thickness according to Eq. (8). However, an increase in the membrane thickness will increase the ohmic loss and thus lower the cell performance.

4.2. Alkali transport through the membrane (alkali crossover)

As mentioned earlier, an alkali has to be introduced into the fuel solution because the ionic conductivity of ion exchange membranes is rather low. In addition to ethanol, the membranes used in alkaline DEFCs are also permeable to alkali so that alkali can transport through the membrane to the cathode (alkali crossover). The presence of alkali will cause two serious issues. First, alkali will react with carbon dioxide from the ambient air to cause carbonation precipitation that potentially blocks the porous structure, hindering transport of various species and reducing the reaction sites [2]. Second, the presence of alkali will change the wettability of the cathode DL, thereby breaking the balance of transport between water and oxygen [21]. As such, the rate of alkali crossover should be decreased to alleviate its negative impact on transport process and cell performance. Like the strategies used to lower the ethanol crossover rate, the rate of the alkali crossover can also be decreased by using the membranes that offer the lower alkali permeability. An et al. [45] measured and compared the

NaOH permeabilities of the three commercial membranes, i.e.: HEM (Tokuyama A201), APM (PBI membrane provided by Yick-Vic) and CEM (Nafion 211). They found that at room temperature, the NaOH permeability of the APM was 1.983×10^{-7} cm^2 s^{-1}, but the values for the both HEM and CEM were relatively lower, i.e.: 2.541×10^{-8} cm^2 s^{-1} and 3.778×10^{-8} cm^2 s^{-1}, respectively. It was explained that the HEM and CEM had functional groups, hindering the ionic transport due to the charge repulsion. Hence, the ion exchange membranes are still preferred from the alkali permeability point of view in this fuel cell system.

4.3. Water transport through the membrane (water crossover)

In addition to ethanol and alkali, water can also transport through the membrane (water crossover). Practically, a diluted fuel will be fed to the anode flow field and as shown by Eq. (1), water is also produced in the anode. It should be noted that as shown by Eq. (3), water is a reactant in the cathode. As such, water crossover is essential in the present fuel cell system, while too much water penetrating to the cathode may lead to the water flooding problem [48]. Hence, how to maintain an appropriate rate of water transport through the membrane is a key transport issue.

Similar to the ethanol crossover, water transport through the membrane is also due to the following three mechanisms.

(i) Diffusion by the water concentration gradient:

$$J_D = D_{w,m} \frac{C_{acl/m} - C_{ccl/m}}{\delta_m} \tag{9}$$

where $D_{w,m}$ is the effective diffusivity of water in the membrane.

(ii) EOD by the hydroxide-ion migration:

$$J_{EOD} = n_d \frac{i}{F} \tag{10}$$

(iii) Convection by the liquid pressure gradient:

$$J_C = \frac{K\rho(p_{acl/m} - p_{ccl/m})}{\mu M_{H_2O} \delta_m} \tag{11}$$

Hence, the total water flux due to the three mechanisms can be expressed

$$J_{wc} = J_D + J_C - J_{EOD} = D_{w,m} \frac{C_{acl/m} - C_{ccl/m}}{\delta_m} + \frac{K\rho(p_{acl/m} - p_{ccl/m})}{\mu M_{H_2O} \delta_m} - n_d \frac{i}{F} \tag{12}$$
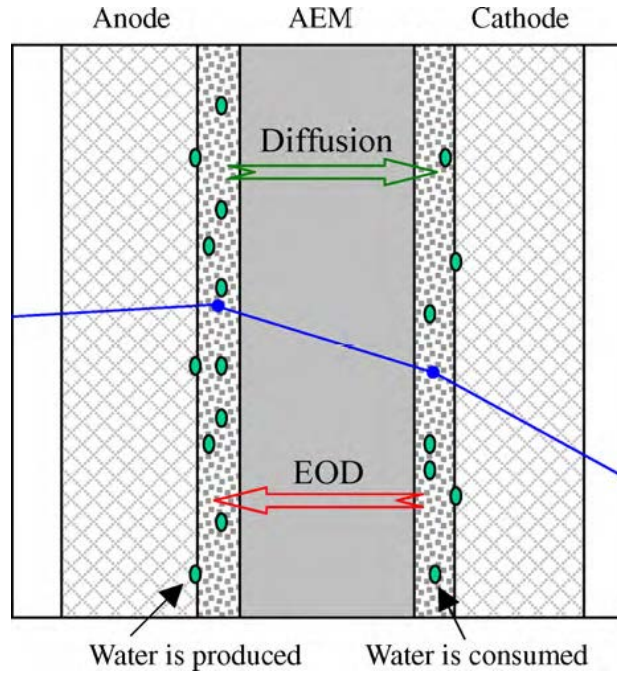
(a)
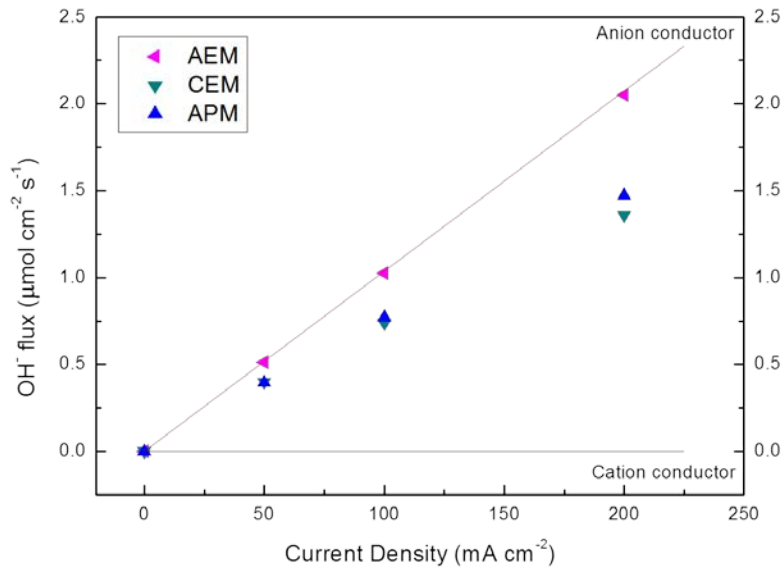
(b)

Fig. 5 (a) The typical water distribution through the fuel cell structure in an alkaline DEFC [48]. (b) Variations in the OH$^-$ flux through three membranes [65].

The water distribution profile through the MEA in an alkaline DEFC is illustrated in Fig. 5a [48]. Recently, Li et al. [48] demonstrated that the cathode flooding also occurred in an alkaline DEFC, because the water flux due to diffusion from the anode to the cathode outweighed the water flux due to both the ORR and EOD. It was also found that unlike in acid fuel cells, the cathode flooding occurred at high current densities, while the cathode flooding occurred at intermediate current densities in alkaline fuel cells. Therefore, a high water crossover rate results in water flooding, increasing transport resistance of oxygen. Hence, how to maintain an appropriate water transport rate through the membrane is a key transport issue. Li et al. [49]

designed an in-situ method to determine the water crossover rate. They termed a net

water flux through the membrane as the water-crossover flux. As part of the

water-crossover flux, J_{wc}, was consumed by the ORR:

$$J_{ORR} = \frac{i}{2F}$$ (13)

while the remaining was removed from the cathode:

$$J_{CDL} = \frac{N_{H_2O}}{A}$$ (14)

Hence, the water-crossover flux was determined:

$$J_{wc} = J_{ORR} + J_{CDL}$$ (15)

Li et al. [49] investigated the effect of the cathode MPL design on the water crossover

rate. It was demonstrated that the presence of a hydrophobic MPL at the cathode

improved the cell performance. In addition, they also investigated the effect of the

carbon nanotube (CNT) loading ranging from 1.0 mg cm^{-2} to 3.0 mg cm^{-2} in the

cathode MPL on the cell performance when the PTFE loading was kept to be 20 wt.

%. It turned out that the best cell performance was achieved at a CNT loading of 2.0

mg cm^{-2}. Similarly, there also existed an optimal PTFE loading in the cathode MPL to

exhibit the highest power density.

In addition, the water crossover rate is also dependent of the water transport

properties of the membranes employed, as illustrated in Eq. (12). Li et al. [51]

measured water transport properties of a commercial HEM (Tokuyama A201), such as

the water diffusivity and the EOD coefficient. It was shown that the Schroeder's

paradox phenomenon was also found to exist in this HEM, and the water diffusivity

of the HEM showed the same order of 10^{-10} m^2 s^{-1} as the Nafion membrane did. In

addition, the EOD coefficients measured at 30°C and 40°C were, respectively, 2.3 and

3.6. Wang et al. [52] investigated the EOD coefficient of a water-vapor equilibrated

HEM (Tokuyama A201), which were determined from the steady-state voltage of a

water concentration cell. They found that the EOD coefficient of the membrane at

room temperature was 0.61 (± 0.12), which was relatively independent of water

content over the relative humidity range of 14% - 96%. Recently, Duan et al. [53]

investigated the water uptake, ionic conductivity and dimensional change of the HEM

(Tokuyama A201) at different temperatures and water activities. They found that the

water uptake increased with the water content and the temperature. In addition, the

water sorption data showed Schroeder's paradox for the HEM.

It should be noted that the above-mentioned transport properties of the membrane

were obtained from the HEM, which was only contacted with liquid water/water

vapor. However, the actual fuel cell operation involves the alkali in the fuel solution,

meaning that the HEM is always immersed in the alkaline solution, rather than the

pure water/water vapor. For this reason, An et al. [45] measured various properties of

the membrane in the alkaline solution, including the ionic conductivity, the liquid

uptake, the species permeability, as well as the thermal and mechanical properties. It was demonstrated that the membrane properties in the alkaline solution were tremendously different from those in the pure water. Huang et al. [54, 55] compared the performance of alkaline DEFCs using different membranes (HEM and non-permselective porous separators). It was found that with a low-cost porous separator, the fuel cell could obtain similar power output as those using expensive HEMs did. Hence, it was concluded that it was feasible to replace the HEM with non-permselective separators.

In summary, the previous investigations suggest that the HEM is still the most promising membrane for the present fuel cell system, although the thermal stability has to be further enhanced.

4.4. Ion transport through the membrane (charge carrier)

In alkaline DEFCs, as an alkali (NaOH/KOH) is mixed with ethanol, both anions (OH$^-$) and cations (Na$^+$/K$^+$) are presented in the fuel cell system [56, 57, 58, 59]. Despite of the fact that there co-existed anions and cations in alkaline DEFCs, most of the previous works [60] employed HEMs or APMs in alkaline DEFCs by assuming that OH$^-$ ions were the charge carriers in HEM-DEFCs and APM-DEFCs. Recently, some investigators proposed to use CEMs as the electrolyte, forming a so-called CEM-DEFC [61]. As intended, it was conventionally thought that charge carriers in

both HEM-DEFCs and APM-DEFCs were OH$^-$ ions [62, 63], whereas the charge carriers in CEM-DEFCs were M$^+$ ions [64]. An et al. [65] designed an experimental setup to determine the charge carriers of alkaline DEFCs with the three types of membrane. It was found that regardless of membranes used, the main charge carrier in three alkaline DEFCs was hydroxide ion, particularly including the CEM-DEFC (see Fig. 5b). It was further suggested that the HEM was still the most promising membrane for the present fuel cell system.

5. Transport phenomena in the cathode

5.1. Oxygen transport in the cathode

Oxygen is fed to the cathode flow channel and transported to the cathode CL, where oxygen will be consumed by the ORR. As a result of the fact that the transport resistance of oxygen is rather low [86, 87], the decrease in the oxygen concentration from the flow channel to the CL is relatively small even at high current densities. An et al. [38] investigated the effect of the oxygen concentration. They compared the polarization curves and cathode overpotentials as operated with the pure oxygen and the air, respectively. It was found that the cell voltage with the pure oxygen was higher than that operated with the air over the whole current density region. It was indicated that the higher oxygen concentration resulted in faster kinetics, lowering the cathode activation loss. It was also found that by using the air, the oxygen

concentration in the cathode CL was almost the same with that in the inlet, indicating the transport rate of oxygen was high enough to match the reaction rate. Modestov et al. [66] fabricated an MEA using non-platinum electrocatalysts and an APM for alkaline DEFCs. The peak power density reached 100 mW cm^{-2} when the cell was operated with the air at ambient pressure. They also found that operating the cell with pure oxygen resulted in about 10% increment of current density. When the fuel cell was passively operated with the ambient air, the so-called air-breathing operation, oxygen was delivered by diffusion and natural convection. In this case, the oxygen transport rate was closely related to the water removal rate, which will be discussed in the following section.

5.2. Water transport in the cathode

On the cathode, the liquid water transport is toward the opposite direction of oxygen transport. As such, two transport processes are intrinsically related to each other. When the liquid water can be effectively removed, oxygen will be sufficiently supplied to reaction sites [86, 87]. Water coming from the anode is consumed in the cathode CL, and then the remaining will be removed from the cathode. As mentioned earlier, the previous studies have shown that the water flooding still occurs in alkaline DEFCs, particularly in the moderate current density region [48]. The water transport through the cathode is primarily driven by the capillary pressure gradient [86]:

$$J_{wr} = -\frac{Ks^3}{\mu_1/\rho_1}\nabla p_1 = (\frac{s^3\sigma\cos(\theta)}{\mu_1/\rho_1}\sqrt{\varepsilon K})\frac{\mathrm{d}J(s)}{\mathrm{d}s}\nabla s \qquad (16)$$

Based on Eq. (16), the liquid water transport in the cathode can be affected by a number of influence factors, such as the wettability, porosity, as well as permeability of the cathode DL.
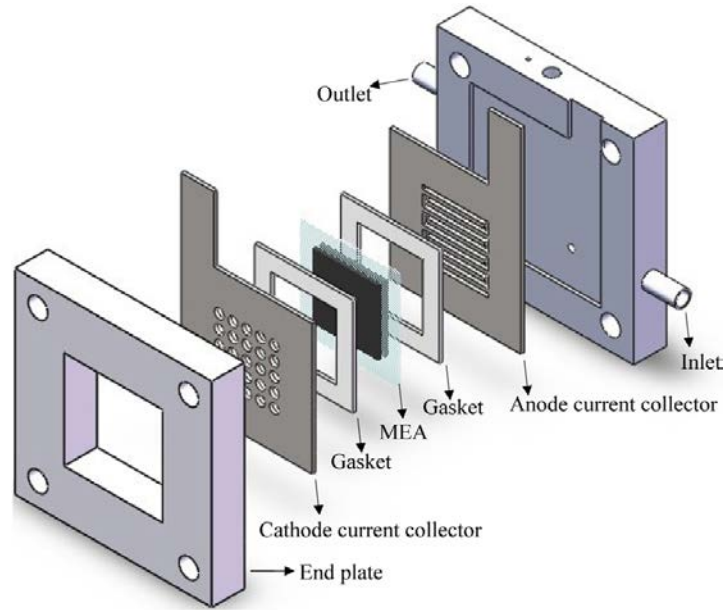
(a)
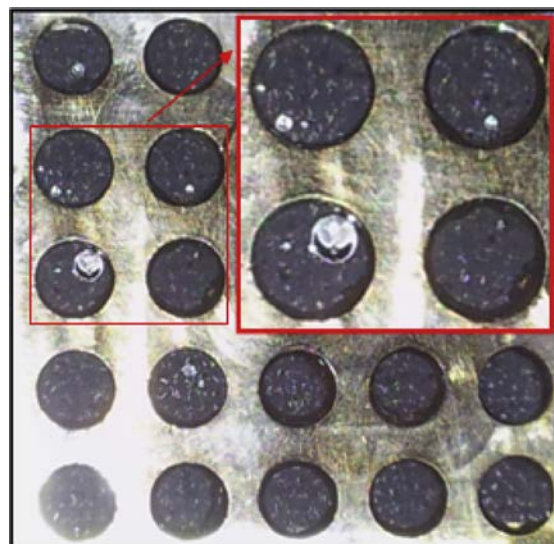
(b)
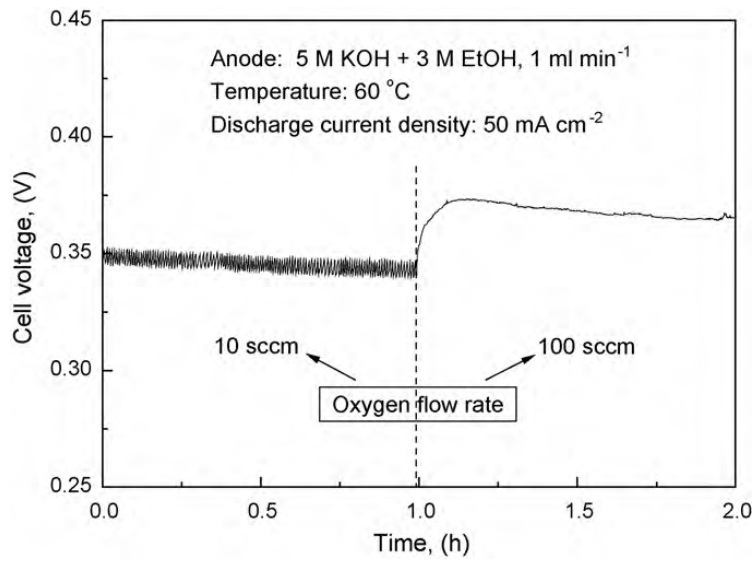
(c)
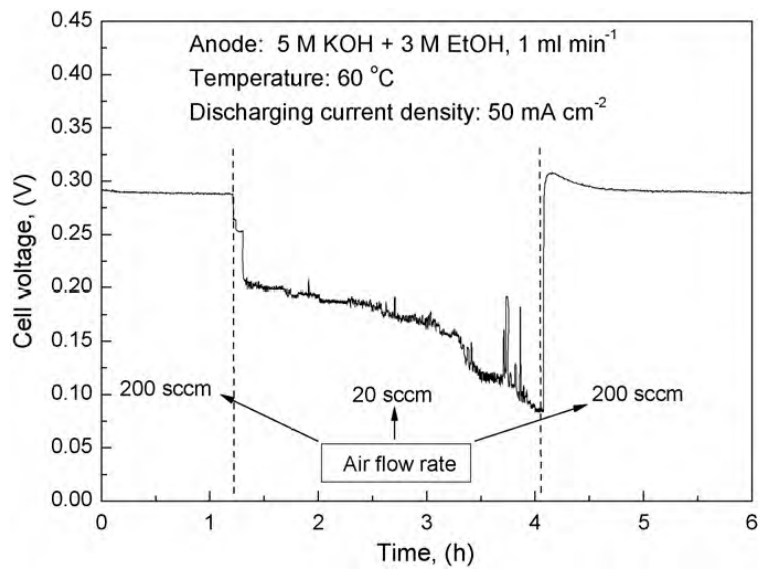
(d)

(a) 10 sccm   (b) 100 sccm
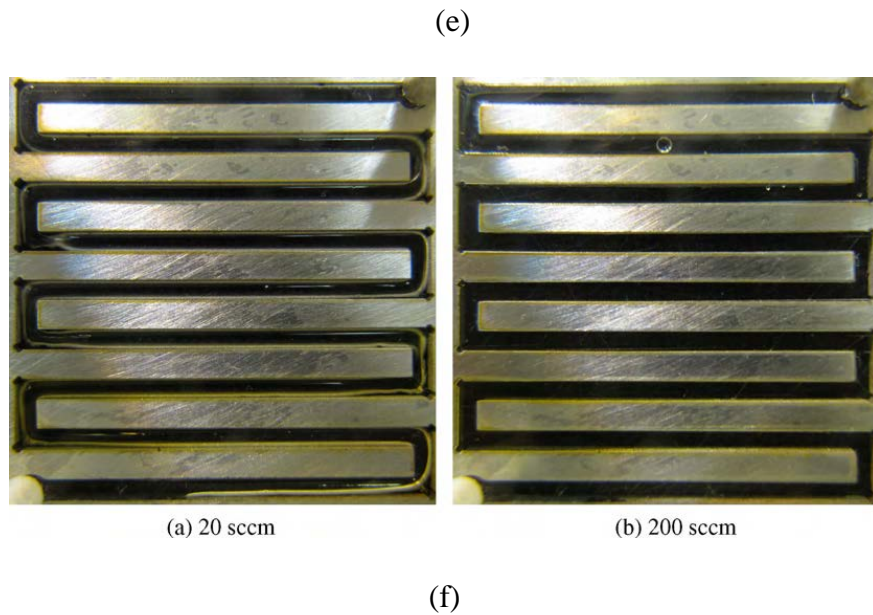
(e)

(a) 20 sccm   (b) 200 sccm

(f)

Fig. 6 (a) Schematic illustration of an air-breathing alkaline DEFC [35]. (b) The water accumulation on the cathode of the air-breathing alkaline DEFC [35]. Effect of the gas flow rate on the transient cell voltage: (c) oxygen; and (d) air [48]. Liquid water flow behaviors: (e) oxygen; and (f) air [48].

5.2.1. Effect of the oxygen delivery mode

Typically, there are two operation modes for the oxygen delivery to the reaction sites: active mode and passive mode (air-breathing). In air-breathing alkaline DEFCs, the removal of water relies on passive forces, such as capillary forces. As such, passively facilitating water and oxygen transport is the key to improve the performance of air-breathing alkaline DEFCs. Li et al. [35] developed and tested an air-breathing alkaline DEFC with Pt-free electrodes, as shown in Fig. 6a. It was revealed that the cathode water flooding behavior occurred in an air-breathing alkaline

DEFC, as shown in Fig. 6b. Radically different from the air-breathing one, the water removal rate was regulated by the gas flow rate in an alkaline DEFC with an active oxygen delivery mode.

5.2.2. Effect of the gas flow rate

Li et al. [24] investigated the effect of oxygen flow rate and found that although not substantial, the cell performance was increased when the oxygen flow rate was increased from 10 sccm to 400 sccm. Also, they measured the transient cell voltage with the oxygen flow rate ranging from 10 sccm to 100 sccm and the air flow rate from 20 sccm to 200 sccm, respectively, as presented in Figs. 6c and 6d [48]. At 10 sccm, the cell voltage underwent significant fluctuations. At 100 sccm, however, the cell voltage became much more stable, as shown in Figs. 6e and 6f. In summary, increasing the gas flow rate is an effective approach to remove the liquid water and thus enhance the transport of oxygen.

5.2.3. Effect of the presence of carbon dioxide

The most challenging issue on the cathode results from the presence of CO_2 when the cell is operated with the ambient air. On one hand, the reaction between CO_2 (extracted from the ambient air) and hydroxide ions (generated by the ORR and penetrated from the anode) produces carbonate, which may replace hydroxide ions as the charge carriers [21]. On the other hand, cations (typically Na^+/K^+) from the anode

will combine with the carbonate to form the carbonation precipitation on the cathode, physically blocking the pores, thus increasing the transport resistance of oxygen [2]. Hence, the problem associated with CO_2 has to be addressed before the alkaline DEFC technology becomes possible. Hou et al. [67] investigated the stability and durability of APM-DEFC operated in the ambient air. It was shown that a 256-h discharging curve with large voltage fluctuations (> 100 mV) during the whole process. They explained that the voltage fluctuation was attributed to the use of the 45 wt. % PtRu/C on the anode, as the large voltage fluctuation phenomenon disappeared when the PtRu/C catalyst was replaced by the Pd/C catalyst. However, it seems that the negative effect of carbon dioxide from the ambient air on the cell performance was missing in their discussion. It should be mentioned that an effective approach is to include an air filter outside of the cathode, separating CO_2 from the air, with which the CO_2-free air can be fed into the cathode.

5.2.4. Effect of the cathode diffusion layer

As mentioned earlier, it is demonstrated that the water flooding also occurs in an alkaline DEFC, significantly increasing the transport resistance of oxygen [48]. As proposed by Li et al. [49], it is essential to incorporate a hydrophobic MPL in the cathode to alleviate the water flooding problem, which is typically composed of carbon materials and polymer binder (typically PTFE). Based on Eq. (16), it is found

that the liquid water removal through the cathode is dependent of the physical properties of the cathode, including the porosity, permeability, pore size distribution and surface wettability. As such, effects of the above-mentioned physical properties on the water removal from the cathode need to be addressed in the future.

5.2.5. Effect of the cathode catalyst layer

Currently, there is no problem associated with ion transport on the anode due to the added alkali in the fuel solution. On the cathode, although the penetrated alkali from the anode could help establish the triple phase boundaries (TPB), the reaction sites cannot be completely used due to the lack of electrolyte in part of the cathode CL. Recently, Li et al. [68] designed the architecture for the cathode of alkaline DEFCs by depositing palladium particles on the cathode MPL via sputtering technique, as presented in Figs. 7a and 7b. This cathode with a Pd loading of 0.035 mg cm^{-2} enabled a peak power density to be 88 mW cm^{-2}, which was even higher than that using a conventional cathode. It is suggested that the sputtering-deposited electrode is more suitable for this fuel cell system.

5.3. Hydrogen peroxide transport in the cathode (hydrogen peroxide as oxidant)

As discussed earlier, it is essential to avoid the presence of CO_2 in the cathode of alkaline DEFCs. An effective approach is to include an air filter outside of the cathode, separating CO_2 from the air, with which the CO_2-free air can be fed into the cathode.

However, the idea of including an air filter will make the fuel cell system bulkier and

increase the design complexity. Alternatively, many efforts have been devoted to the

development of fuel cells that use hydrogen peroxide as oxidant and significant

progress has been made [69-74].
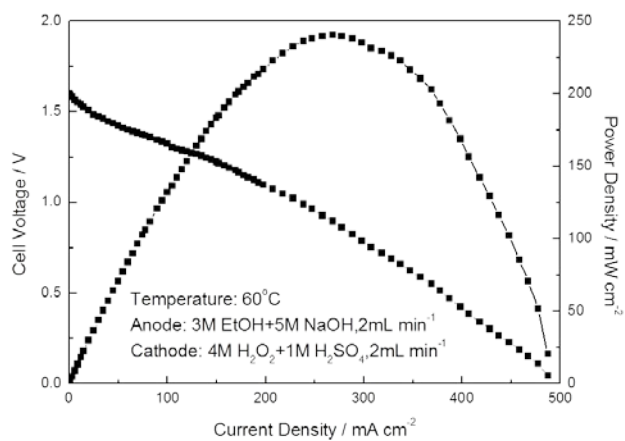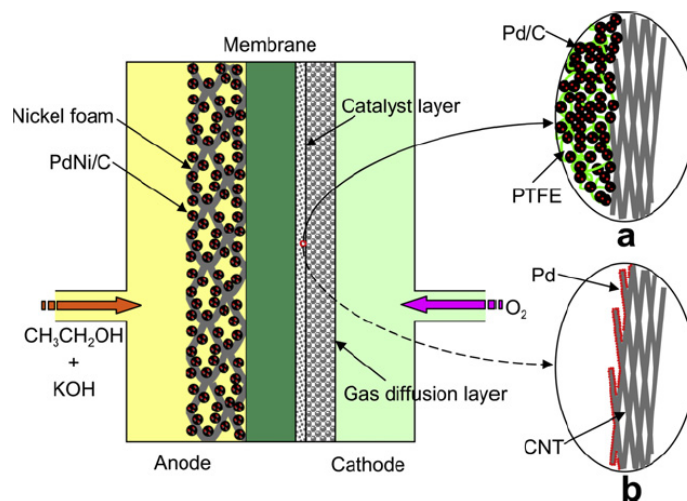
(c)
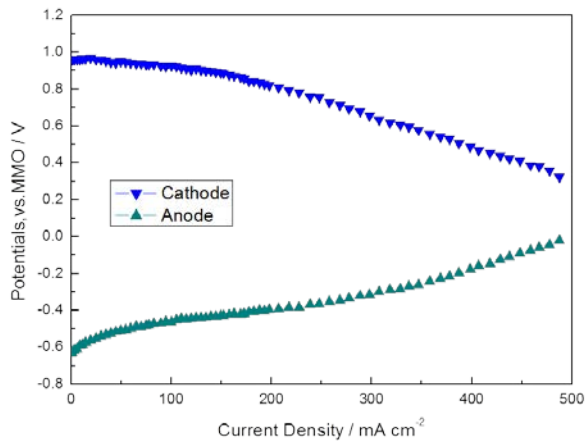
(d)

Fig. 7 Cathode structures: (a) the conventional one; and (b) the sputtering-deposited one [68]; (c) polarization and power density curves; and (d) anode and cathode potentials [76].

For example, An et al. [75] proposed an alkaline DEFC with hydrogen peroxide as oxidant. The fuel cell consisted of a non-platinum anode, an HEM, and a non-platinum cathode. The developed fuel cell not only avoided the carbonation problem encountered in alkaline fuel cells using the ambient air as oxidant, but also yielded a peak power density of 130 mW cm^{-2} at 60°C. As a result of the fact that hydrogen peroxide is not stable in alkaline media, an acid is generally added in the aqueous solution to stabilize the hydrogen peroxide [7]. To this end, An et al. [76] proposed a so-called alkaline-acid DEFC (AA-DEFC) with alkalized ethanol as fuel and acidified hydrogen peroxide as oxidant. It was shown that the theoretical voltage

of this fuel cell was 2.52 V, while it was experimentally demonstrated that this fuel

cell yielded an open-circuit voltage (OCV) of 1.60 V and a peak power density of 240

mW cm^{-2} at 60°C, as shown in Figs. 7c and 7d. The large difference between the

actual OCV and theoretical voltage was mainly caused by the mixed potential

phenomenon occurring on the cathode, which has been substantially discussed in a

previous review paper [77]. Recently, An et al. [78, 79] proposed an approach to avoid

the mixed-potential phenomenon. In this approach, they created the cathode potential

by introducing a redox couple to the cathode while using hydrogen peroxide to

chemically charge the redox ions, as illustrated in Figs. 8a and 8b.
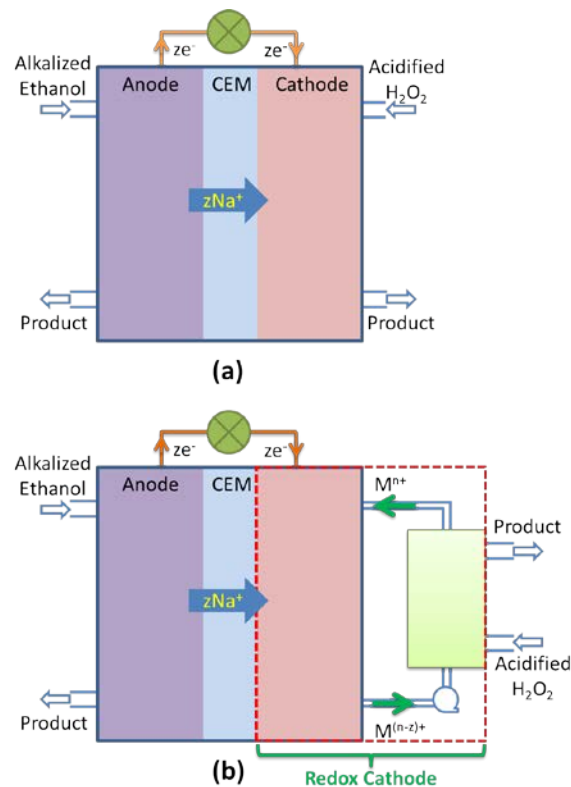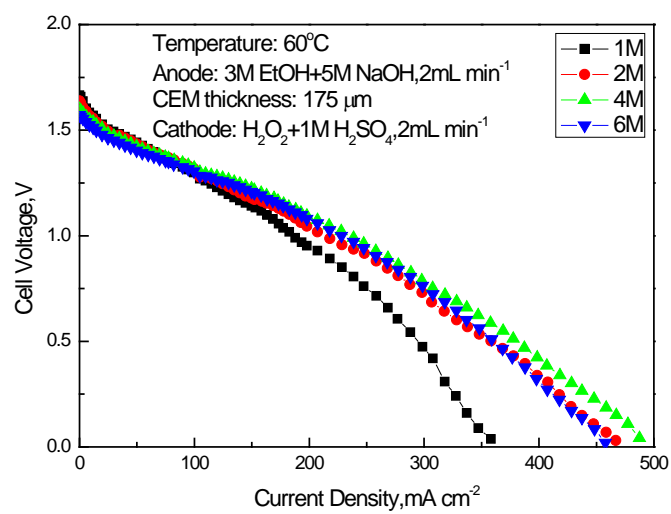
(c)
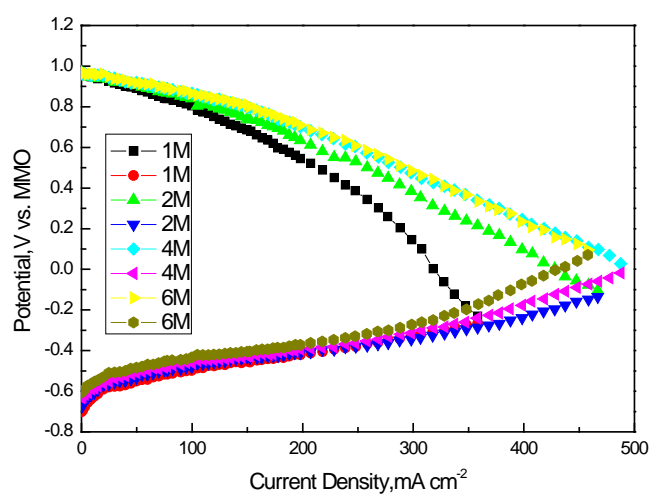
(d)
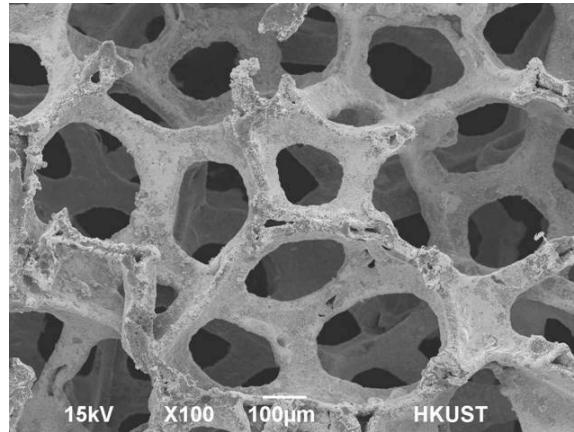
(e)
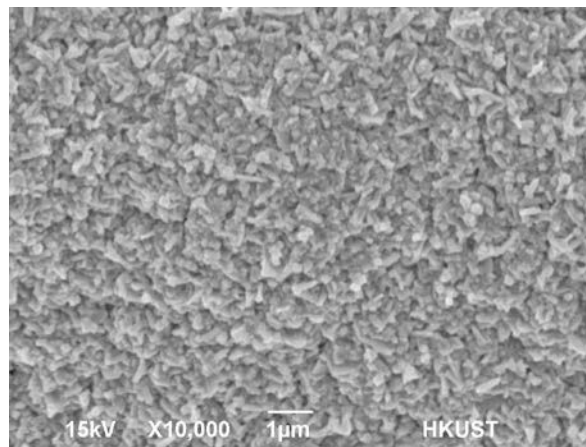
(f)

Fig. 8 (a) Conventional and (b) mixed-potential-free hydrogen peroxide fuel cells [78].

Effect of the hydrogen peroxide concentration: (c) polarization curves; (d) anode and

cathode potentials [80]. The SEM images of the bi-functional electrode: (e) 3-D

structure; and (f) surface morphology [85].

Similarly, hydrogen peroxide in the catholyte flows into the cathode flow channel

and transports through the cathode DL to the cathode CL. Hence, the operating and

electrode structural design parameters in the cathode can affect the transport process

of hydrogen peroxide. Similarly, it is also critically important to maintain an appropriate concentration of hydrogen peroxide in the cathode CL.

5.3.1. Effect of the hydrogen peroxide concentration

The hydrogen peroxide concentration in the catholyte is an important parameter to achieve an appropriate concentration of hydrogen peroxide in the cathode CL. An et al. [75] investigated the effect of the hydrogen peroxide concentration on the performance in an alkaline DEFC. It was shown that the 2.0-M operation resulted in a limiting current density, which was disappeared at 4.0-M operation. A further increase to 8.0 M did not change the cell performance as the hydrogen peroxide concentration was sufficient for the reaction rate. Recently, An et al. [80] further investigated the effect of the hydrogen peroxide concentration on the performance of an AA-DEFC using the acidified hydrogen peroxide as oxidant, as shown in Figs. 8c and 8d. It was found that when the hydrogen peroxide concentration was increased from 1.0 M to 4.0 M, the transport of hydrogen peroxide at the cathode was correspondingly enhanced, reducing the concentration loss of hydrogen peroxide. A further increase to 6.0 M slightly decreased the performance. It was indicated that the hydrogen peroxide concentration in the cathode CL was sufficient, but the high hydrogen peroxide concentration caused rather serious hydrogen peroxide crossover, thereby decreasing the cell performance.

5.3.2. Effect of the cathode electrode design

As mentioned earlier, the oxygen evolution from the hydrogen peroxide decomposition not only significantly increases the transport of hydrogen peroxide to reaction sites, but also decreases the utilization efficiency of hydrogen peroxide. The mechanisms leading to the hydrogen peroxide decomposition have been extensively investigated and some strategies have been proposed to alleviate or even avoid the hydrogen peroxide decomposition [82-85]. An et al. [85] developed a bi-functional electrode, which was composed of the nickel-chromium foam (functioning as the DL) with highly dispersed gold particles (functioning as the CL) deposited onto the skeleton of the foam, as shown in Figs. 8e and 8f. This electrode allowed not only a reduction in the decomposition rate of hydrogen peroxide, but also an increase in the transport rate of hydrogen peroxide. The performance test showed that the use of this electrode increased the peak power density from 135 mW cm^{-2} to 200 mW cm^{-2}. It is suggested that this bi-functional electrode is more suitable for the fuel cell system that operates with hydrogen peroxide.

6. Mathematical modeling of alkaline DEFCs

As mentioned earlier, the alkaline DFFC system has a complex multi-layered porous structure, in which the coupled mass/charge transport and electrochemical reactions take place simultaneously. Hence, it is difficult to shed light on the complicated

physicochemical processes via experimental investigations. The mathematical modeling, as a powerful and economical tool, plays an important role in quantifying the physicochemical processes in fuel cells. For this reason, a few numerical investigations have been conducted to study the transport processes in alkaline DEFCs [38, 47, 55]. Mathematical models for alkaline DEFCs are generally developed based on single-phase mass transport. Bahrami et al. [47] developed a one-dimensional model to study the transport process in an alkaline DEFC incorporating an HEM. Particularly, they proposed a multi-layer membrane model to determine the diffusive and electro-osmotic transport of ethanol. They investigated the ethanol crossover for positive and negative EOD coefficients, respectively, and found that a substantial difference in ethanol distribution in the membrane. Also, the ethanol crossover rate was significantly reduced when using an HEM instead of a PEM, particularly at current densities higher than 500 A m^{-2}. Hence, the EOD direction from the cathode to the anode much decreases the ethanol permeation rate. Huang et al. [55] developed a physical model to investigate the transport processes in an alkaline DEFC using a non-permselective separator. It was found that the alkali concentration lower than 1.0 M notably decreased cell performance due to the low electrolyte conductivity. The above mathematical models of alkaline DEFCs indicate that the performance of an alkaline DEFC is affected by the structural design and operating parameters.

7. Concluding remarks

As a relatively new field, the alkaline DEFC technology has undergone a rapid progress in the past decade. This article provides a comprehensive review of transport phenomena in the alkaline DEFC system. Particular attention is paid to the mechanisms and the critical issues of transport of various species through the fuel cell structure. The past investigations have laid a solid foundation for the basic understanding of how the structural design parameters of membrane electrode assemblies and the operating parameters affect the fuel cell performance. The critical transport issues that need to be further addressed in the near future include:

1) Ethanol transport: Maintaining an appropriate ethanol concentration level in the anode CL is the direction to maximize the cell performance.

2) Water transport: The direction of water management is to transport water through the membrane to the cathode at an appropriate rate.

3) Alkali transport: The direction of alkali management is to alleviate or eliminate the alkali crossover.

4) Carbon dioxide: When the air is used as oxidant, CO_2 from the air can react with hydroxide ions generated by the ORR and penetrated from the anode to form carbonate, limiting the fuel cell performance and durability.

5) Oxygen transport: The direction of oxygen transport is how to enhance the oxygen

supply to the cathode catalyst layer and the water removal from the cathode diffusion layer by utilizing passive forces or regulating the gas flow rates.

6) Hydrogen peroxide transport: Maintaining an appropriate hydrogen peroxide concentration level in the cathode CL is the direction to maximize the cell performance. On the other hand, the issue associated with hydrogen peroxide decomposition has to be addressed before the fuel cell technology using hydrogen peroxide as oxidant becomes possible; the rate of hydrogen peroxide decomposition can be reduced by optimizing the pH value, the hydrogen peroxide concentration, the temperature of the aqueous solution, and the electrochemical properties of electrode materials.

Acknowledgements

References

[1] E. Antolini, Palladium in fuel cell catalysis, Energy Environ. Sci. 2 (2009) 915-931.

[2] T.S. Zhao, Y.S. Li, S.Y. Shen, Anion-exchange membrane direct ethanol fuel cells: Status and perspective, Front. Energy Power Eng. China 4 (2010) 443-458.

[3] C. Bianchini, P.K. Shen, Palladium-based electrocatalysts for alcohol oxidation in half cells and in direct alcohol fuel cells, Chem. Rev. 109 (2009) 4183-4206.

[4] S.Y. Shen, T.S. Zhao, One-step polyol synthesis of Rh-on-Pd bimetallic nanodendrites and their electrocatalytic properties for ethanol oxidation in alkaline media, J. Mater. Chem. A 1 (2013) 906-912.

[5] E.H. Yu, X. Wang, U. Krewer, L. Li, K. Scott, Direct oxidation alkaline fuel cells: from materials to systems, Energy Environ. Sci. 5 (2012) 5668-5680.

[6] V. Rao, Hariyanto, C. Cremers, U. Stimming, Investigation of the ethanol electro-oxidation in alkaline membrane electrode assembly by differential electrochemical mass spectrometry, Fuel Cells 7 (2007) 417-423.

[7] W.J. Zhou, S.Q. Song, W.Z. Li, Z.H. Zhou, G.Q. Sun, Q. Xin, S. Douvartzides, P. Tsiakaras, Direct ethanol fuel cells based on PtSn anodes: the effect of Sn content on the fuel cell performance, J. Power Sources 140 (2005) 50-58.

[8] L. Wang, A. Lavacchi, M. Bevilacqua, M. Bellini, P. Fornasiero, J. Filippi, M. Innocenti, A. Marchionni, H.A. Miller, F. Vizza, Energy efficiency of alkaline direct ethanol fuel cells empolying nanostructured palladium electrocatalysts, ChemCatChem 7 (2015) 2214-2221.

[9] S.J. Guo, S.J. Dong, E.K. Wang, Pt/Pd bimetallic nanotubes with petal-like surfaces for enhanced catalytic activity and stability towards ethanol electrooxidation, Energy Environ. Sci. 3 (2010) 1307-1310.

[10] E. Antolini, E.R. Gonzalez, Alkaline direct alcohol fuel cells, J. Power Sources 195 (2010) 3431-3450.

[11] E.H. Yu, U. Krewer, K. Scott, Principles and Materials Aspects of Direct Alkaline Alcohol Fuel Cells, Energies 3 (2010) 1499-1528.

[12] L. Zeng, T.S. Zhao, L. An, A high-performance supportless silver nanowire catalyst for anion exchange membrane fuel cells, J. Mater. Chem. A 3 (2015) 1410-1416.

[13] J.S. Spendelow, A. Wieckowski, Electrocatalysis of oxygen reduction and small alcohol oxidation in alkaline media, Phys. Chem. Chem. Phys. 9 (2007) 2654-2675.

[14] N.J. Robertson, H.A.K. IV, T.J. Clark, P.F. Mutolo, H.D. Abruna, G.W. Coates, Tunable High Performance Cross-Linked Alkaline Anion Exchange Membranes for Fuel Cell Applications, J. Am. Chem. Soc. 132 (2010) 3400-3404.

[15] F. Ksar, L. Ramos, B. Keita, L. Nadjo, P. Beaunier, H. Remita, Bimetallic Palladium-Gold Nanostructures: Application in Ethanol Oxidation, Chem. Mater. 21 (2009) 3677-3683.

[16] L. An, T.S. Zhao, Z.H. Chai, P. Tan, L. Zeng, Mathematical modeling of an anion-exchange membrane water electrolyzer for hydrogen production, Int. J. Hydrogen Energy 39 (2014) 19869-19876.

[17] Y.S. Li, T.S. Zhao, Z.X. Liang, Effect of polymer binders in anode catalyst layer on performance of alkaline direct ethanol fuel cells, J. Power Sources 190 (2009) 223-229.

[18] J.R. Varcoe, R.C.T. Slade, Prospects for alkaline anion-exchange membranes in low temperature fuel cells, Fuel Cells 5 (2005) 187-200.

[19] C. Bianchini, P.K. Shen, Palladium-based electrocatalysts for alcohol oxidation in half cells and in direct alcohol fuel cells, Chem. Rev. 109 (2009) 4183-4206.

[20] J.B. Xu, T.S. Zhao, Y.S. Li, W.W. Yang, Synthesis and characterization of the Au-modified Pd cathode catalyst for alkaline direct ethanol fuel cells, Int. J. Hydrogen Energy 35 (2010) 9693-9700.

[21] L. An, T.S. Zhao, Y.S. Li, Carbon-neutral sustainable energy technology: Direct ethanol fuel cells, Renewable and Sustainable Energy Reviews 50 (2015) 1462-1468.

[22] L. An, T.S. Zhao, S.Y. Shen, Q.X. Wu, R. Chen, Performance of a direct ethylene glycol fuel cell with an anion-exchange membrane, Int. J. Hydrogen Energy 35 (2010)

4329-4335.

[23] L. An, T.S. Zhao, S.Y. Shen, Q.X. Wu, R. Chen, An alkaline direct oxidation fuel cell with non-platinum catalysts capable of converting glucose to electricity at high power output, J. Power Sources 196 (2011) 186-190.

[24] Y.S. Li, T.S. Zhao, Z.X. Liang, Performance of alkaline electrolyte-membrane based direct ethanol fuel cells, J. Power Sources 187 (2009) 387-392.

[25] E.H. Yu, U. Krewer, K. Scott, Principles and Materials Aspects of Direct Alkaline Alcohol Fuel Cells, Energies 3 (2010) 1499-1528.

[26] E. Antolini, Catalysts for direct ethanol fuel cells, J. Power Sources 170 (2007) 1-12.

[27] E. Antolini, E.R. Gonzalezb, Alkaline direct alcohol fuel cells, J. Power Sources 195 (2010) 3431-3450.

[28] M.Z.F. Kamarudin, S.K. Kamarudin, M.S. Masdar, W.R.W. Daud, Review: Direct ethanol fuel cells, Int. J. Hydrogen Energy 38 (2013) 9438-9453.

[29] C. Bianchini, P.K. Shen, Palladium-based electrocatalysts for alcohol oxidation in half cells and in direct alcohol fuel cells, Chem. Rev. 109 (2009) 4183-4206.

[30] E.H. Yu, X. Wang, U. Krewer, L. Lid, K. Scotta, Direct oxidation alkaline fuel cells: from materials to systems, Energy Environ. Sci. 5 (2012) 5668-5680.

[31] A. Brouzgou, A. Podias, P. Tsiakaras, PEMFCs and AEMFCs directly fed with ethanol: a current status comparative review, J. Appl Electrochem 43 (2013) 119-136.

[32] J.R. Varcoe, R.C.T. Slade, Prospects for Alkaline Anion-Exchange Membranes in Low Temperature Fuel Cells, Fuel Cells 5 (2005) 187-200.

[33] J.R. Varcoe, P. Atanassov, D.R. Dekel, A.M. Herring, M.A. Hickner, P.A. Kohl, A.R. Kucernak, W.E. Mustain, K. Nijmeijer, K. Scott, T.W. Xu, L. Zhuang,

Anion-exchange membranes for electrochemical energy systems, Energy Environ. Sci. 7 (2014) 3135-3191.

[34] S.P.S. Badwal, S. Giddey, A. Kulkarni, J. Goel, S. Basu, Direct ethanol fuel cells for transport and stationary applications – A comprehensive review, Applied Energy 145 (2015) 80-103.

[35] Y.S. Li, Y.L. He, W.W. Yang, Performance characteristics of air-breathing anion-exchange membrane direct ethanol fuel cells, Int. J. Hydrogen Energy 38 (2013) 13427-13433.

[36] Y.S. Li, T.S. Zhao, A high-performance integrated electrode for anion-exchange membrane direct ethanol fuel cells, Int. J. Hydrogen Energy 36 (2011) 7707-7713.

[37] R.W. Verjulio, F. Álcaide, G. Alvarez, N. Sabaté, N. Torres-Herrero, J.P. Esquivel, J. Santander, A micro alkaline direct ethanol fuel cell with platinum-free catalysts, J. Micromech. Microeng. 23 (2013) 1-7.

[38] L. An, Z.H. Chai, L. Zeng, P. Tan, T.S. Zhao, Mathematical modeling of alkaline direct ethanol fuel cells, Int. J. Hydrogen Energy 38 (2013) 14067 -14075.

[39] R. Chetty, K. Scott, Direct ethanol fuel cells with catalysed metal mesh anodes, Electrochimica Acta 52 (2007) 4073-4081.

[40] Y.L. Wang, Y.Q. Zhao, C.L. Xu, D.D. Zhao, M.W. Xu, Z.X. Su, H.L. Li, Improved performance of Pd electrocatalyst supported on three-dimensional nickel foam for direct ethanol fuel cells, J. Power Sources 195 (2010) 6496-6499.

[41] J.R. Varcoe, R.C.T. Slade, E.L.H. Yee, S.D. Poynton, D.J. Driscoll, Investigations into the ex situ methanol, ethanol and ethylene glycol permeabilities of alkaline polymer electrolyte membranes, J. Power Sources 173 (2007) 194-199.

[42] H.Y. Hou, G.Q. Sun, R.H. He, Z.M. Wu, B.Y. Sun, Alkali doped polybenzimidazole membrane for high performance alkaline direct ethanol fuel cell, J.

Power Sources 182 (2008) 95-99.

[43] A.Y. Leykina, O.A. Shkrebko, M.R. Tarasevich, Ethanol crossover through alkali-doped polybenzimidazole membrane, J. Membrane Science 328 (2009) 86-89.

[44] H. Jung, K. Fujii, T. Tamaki, H. Ohashi, T. Ito, T. Yamaguchi, Low fuel crossover anion exchange pore-filling membrane for solid-state alkaline fuel cells, J. Membrane Science 373 (2011) 107-111.

[45] L. An, T.S. Zhao, Q.X. Wu, L. Zeng, 2012, Comparison of different types of membrane in alkaline direct ethanol fuel cells, Int. J. Hydrogen Energy 37 (2012) 14536-14542.

[46] S.Q. Song, W.J. Zhou, Z.X. Liang, R. Cai, G.Q. Sun, Q. Xin, The effect of methanol and ethanol cross-over on the performance of PtRu/C-based anode DAFCs, Appl Catal. B Environ. 55 (2005) 65-72.

[47] H. Bahrami, A. Faghri, Multi-layer membrane model for mass transport in a direct ethanol fuel cell using an alkaline anion exchange membrane, J. Power Sources 218 (2012) 286-296.

[48] Y.S. Li, T.S. Zhao, R. Chen, Cathode flooding behavior in alkaline direct ethanol fuel cells, J. Power Sources 196 (2011) 133-139.

[49] Y.S. Li, T.S. Zhao, J.B. Xu, S.Y. Shen, W.W. Yang, Effect of the cathode micro-porous layer on performance of anion-exchange membrane direct ethanol fuel cells, J. Power Sources 196 (2011) 1802-1807.

[50] Q.X. Wu, T.S. Zhao, R. Chen, W.W. Yang, Effects of anode microporous layers made of carbon powder and nanotubes on water transport in direct methanol fuel cells, J. Power Sources 191 (2009) 304-311.

[51] Y.S. Li, T.S. Zhao, W.W. Yang, Measurements of water uptake and transport properties in anion-exchange membranes, Int. J. Hydrogen Energy 35 (2010) 5656-5665.

[52] X.H. Wang, J.P. McClure, P.S. Fedkiw, Transport properties of proton- and hydroxide-exchange membranes for fuel cells, Electrochim. Acta 79 (2012) 126-132.

[53] Q.J. Duan, S.H. Ge, C.Y. Wang, Water uptake, ionic conductivity and swelling properties of anion-exchange membrane, J. Power Sources 243 (2013) 773-778.

[54] J. Huang, A. Faghri, Comparison of Alkaline Direct Ethanol Fuel Cells With and Without Anion Exchange Membran, Journal of Fuel Cell Science and Technology 11 (2014) 051007.

[55] J. Huang, H. Bahrami, A. Faghri, Analysis of a Permselective Membrane-Free Alkaline Direct Ethanol Fuel Cell, Journal of Fuel Cell Science and Technology 11 (2014) 021009.

[56] M.A. Hickner, H. Ghassemi, Y.S. Kim, B.R. Einsla, J.E. McGrath, Alternative polymer systems for proton exchange membranes (PEMs), Chem. Rev. 104 (2004) 4587-4612.

[57] J.R. Varcoe, R.C.T. Slade, Prospects for alkaline anion-exchange membranes in low temperature fuel cells, Fuel Cells 5 (2005) 187-200.

[58] L. An, L. Zeng, T.S. Zhao, An alkaline direct ethylene glycol fuel cell with an alkali-doped polybenzimidazole membrane, Int. J. Hydrogen Energy 38 (2013) 10602-10606.

[59] L. An, T.S. Zhao, L. Zeng, Agar chemical hydrogel electrode binder for fuel-electrolyte-fed fuel cells, Applied Energy 109 (2013) 67-71.

[60] H. Hou, S. Wang, W. Jin, Q. Jiang, L. Sun, L. Jiang, G. Sun, KOH modified Nafion 112 membrane for high performance alkaline direct ethanol fuel cell, Int. J.

Hydrogen Energy 36 (2011) 5104-5109.

[61] L. An, T.S. Zhao, An alkaline direct ethanol fuel cell with a cation exchange membrane, Energy Environ. Sci. 4 (2011) 2213-2217.

[62] N. Fujiwara, Z. Siroma, S. Yamazaki, T. Ioroi, H. Senoh, K. Yasuda, Direct ethanol fuel cells using an anion exchange membrane, J. Power Sources 185 (2008) 621-626.

[63] B. Xing, O. Savadogo, Hydrogen/oxygen polymer electrolyte membrane fuel cells (PEMFCs) based on alkaline-doped polybenzimidazole (PBI), Electrochem. Commun. 2 (2000) 697-702.

[64] Z.P. Li, B.H. Liu, K. Arai, S. Suda, A fuel cell development for using borohydrides as the fuel, J. Electrochem. Soc. 150 (2003) A868-A872.

[65] L. An, T.S. Zhao, Y.S. Li, Q.X. Wu, Charge carriers in alkaline direct oxidation fuel cells, Energy & Environmental Science 5 (2012) 7536-7538.

[66] A.D. Modestov, M.R. Tarasevich, A.Y. Leykin, V.Y. Filimonov, MEA for alkaline direct ethanol fuel cell with alkali doped PBI membrane and non-platinum electrodes, J. Power Sources 188 (2009) 502-506.

[67] H.Y. Hou, S.L. Wang, Q. Jiang, W. Jin, L.H. Jiang, G.Q. Sun, Durability study of KOH doped polybenzimidazole membrane for air-breathing alkaline direct ethanol fuel cell, J. Power Sources 196 (2011) 3244-3248.

[68] Y.S. Li, T.S. Zhao, Ultra-low loading catalyst cathode electrode for anion-exchange membrane fuel cells, Int. J. Hydrogen Energy 37 (2012) 15334-15338.

[69] J. Ma, N.A. Choudhury, Y. Sahai, A comprehensive review of direct borohydride fuel cells, Rene. Sust. Energy Rev. 14 (2010) 183-199.

[70] L. An, T.S. Zhao, Z.H. Chai, L. Zeng, P. Tan, Modeling of the mixed potential in

hydrogen peroxide-based fuel cells, Int. J. Hydrogen Energy 39 (2014) 7407-7416.

[71] G.H. Miley, N. Luo, J. Mather, Direct $NaBH_4/H_2O_2$ fuel cells, J. Power Sources 165 (2007) 509-516.

[72] N.A. Choudhury, R.K. Raman, S. Sampath, A.K. Shukla. An alkaline direct borohydride fuel cell with hydrogen peroxide as oxidant, J. Power Sources 143 (2005) 1-8.

[73] Y. Yamada, Y. Fukunishi, S. Yamazaki, Hydrogen peroxide as sustainable fuel: electrocatalysts for production with a solar cell and decomposition with the fuel cell, Chem. Commun. 46 (2010) 7334-7336.

[74] N. Luo, G.H. Miley, K.J. Kim, $NaBH_4/H_2O_2$ fuel cells for air independent power systems, J. Power Sources 185 (2008) 685-690.

[75] L. An, T.S. Zhao, L. Zeng, X.H. Yan, Performance of an alkaline direct ethanol fuel cell with hydrogen peroxide as oxidant, Int. J. Hydrogen Energy 39 (2014) 2320-2324.

[76] L. An, T.S. Zhao, R. Chen, Q.X. Wu, A novel direct ethanol fuel cell with high power density, J. Power Sources 196 (2011) 6219–6222.

[77] L. An, T.S. Zhao, X.H. Yan, X.L. Zhou, P. Tan, The dual role of hydrogen peroxide in fuel cells, Science Bulletin 60 (2015) 55-64.

[78] L. An, T.S. Zhao, X.L. Zhou, L. Wei, X.H. Yan, A high-performance ethanol-hydrogen peroxide fuel cell, RSC Advances 4 (2014) 65031-65034.

[79] L. An, T.S. Zhao, X.L. Zhou, X.H. Yan, C.Y. Jung, A low-cost, high-performance zinc–hydrogen peroxide fuel cell, J. Power Sources 275 (2015) 831-834.

[80] L. An, T.S. Zhao, Performance of an alkaline-acid direct ethanol fuel cell, Int. J. Hydrogen Energy 36 (2011) 9994-9999.

[81] M.E. Nolan, A.B. Laconti, Integrated electrochemical-chemical oxygen

generating system, US 4,488,951 (Dec. 18, 1984)

[82] G.H. Miley, N. Luo, J. Mather, R. Burton, G. Hawkins, L. Gu, E. Byrd, R. Gimlin, P.J. Shrestha, G. Benavides, J. Laystrom, D. Carroll, Direct $NaBH_4/H_2O_2$ fuel cells, J. Power Sources 165 (2007) 509-516.

[83] R.K. Raman, N.A. Choudhury, A.K. Shukla, A high output voltage direct borohydride fuel cell, Electrochem. Solid-State Lett. 7 (2004) A488-A491.

[84] W.Q. Yang, S.H. Yang, W. Sun, G.Q. Sun, Q. Xin Q, Nanostructured palladium-silver coated nickel foam cathode for magnesium–hydrogen peroxide fuel cells, Electrochim. Acta 52 (2006) 9-14.

[85] L. An, T.S. Zhao, J.B. Xu, A bi-functional cathode structure for alkaline-acid direct ethanol fuel cells, Int. J. Hydrogen Energy 36 (2011) 13089-13095.

[86] T.S. Zhao, C. Xu, R. Chen, W.W. Yang, Mass transport phenomena in direct methanol fuel cells, Progress in Energy and Combustion Science 35 (2009) 275–292.

[87] T.S. Zhao, R. Chen, W.W. Yang, C. Xu, Small direct methanol fuel cells with passive supply of reactants, J. Power Sources 191 (2009) 185–202.

Figure captions:

Fig. 1 A typical alkaline direct ethanol fuel cell.

Fig. 2 Effect of the ethanol concentration on the cell performance: (a) 1.0 M KOH; (b) 5.0 M KOH [24]. (c) The fabricated micro-DEFC via using micro-technologies: (1) Si-based current collector; (2) micro-fabricated channels; (3) methacrylate case holder; and (4) MEA [37] (Reproduced with permission from IOP Publishing).

Fig. 3 Effect of structural parameters on the performance: (a) thickness; (b) porosity [38]. Anode structures: (c) the conventional one; and (d) the integrated one [36].

Fig. 4 A three-dimensional Pd electrode [40].

Fig. 5 (a) The typical water distribution through the fuel cell structure in an alkaline DEFC [48]. (b) Variations in the OH- flux through three membranes [65].

Fig. 6 (a) Schematic illustration of an air-breathing alkaline DEFC [35]. (b) The water accumulation on the cathode of the air-breathing alkaline DEFC [35]. Effect of the gas flow rate on the transient cell voltage: (c) oxygen; and (d) air [48]. Liquid water flow behaviors: (e) oxygen; and (f) air [48].

Fig. 7 Cathode structures: (a) the conventional one; and (b) the sputtering-deposited one [68]; (c) polarization and power density curves; and (d) anode and cathode potentials [76].

Fig. 8 (a) Conventional and (b) mixed-potential-free hydrogen peroxide fuel cells [78].

Effect of the hydrogen peroxide concentration: (c) polarization curves; (d) anode and cathode potentials [80]. The SEM images of the bi-functional electrode: (e) 3-D structure; and (f) surface morphology [85].

Highlights

- This article provides a review of transport phenomena in ADEFCs.

- Particular attention is paid to mechanisms and critical issues of species transport.

- How structural design and operating parameters affect performance is discussed.

- Future perspectives and challenges with regard to transport are highlighted.

Graphical Abstract: This article provides a comprehensive review of transport phenomena of various species in alkaline direct ethanol fuel cells.

Anode Flow Field

Anode Diffusion Layer

Anode Catalyst Layer

Hydroxide Exchange Membrane

Cathode Catalyst Layer

Cathode Diffusion Layer

Cathode Flow Field